ENHANCED SAFEGUARDS: THE ROLE OFSMART FUNCTIONAL COATINGS FOR TAMPER INDICATION

A.E. Méndez Torres, M. J. Martínez-Rodríguez, K. Brinkman, D. Krementz
Savannah River National Laboratory
Aiken SC, 29808

ABSTRACT

This work investigates the synthesis of smart functional coatings (SFC) using chemical solution deposition methods. Chemical solution deposition methods have recently received attention in the materials research community due to several unique advantages that include low temperature processing, high homogeneity of final products, the ability to fabricate materials with controlled surface properties and pore structures, and the ease of dopant incorporation in controlled concentrations. The optical properties of thin films were investigated using UV-Vis spectroscopy, Raman, SEM and EDS, with the aim of developing a protective transparent coating for a ceramic surface as a first line of defense for tamper indication. The signature produced by the addition of rare earth dopants will be employed as an additional tamper indicating feature. The integration of SFC's as part of a broader verification system such as an electronic seals can provide additional functionality and defense in depth. SFC's can improve the timeliness of detection by providing a robust, in-situ verifiable tamper indication framework.

INTRODUCTION

The IAEA has recognized the need for the development and implementation of advanced authentication, verification, unique identification (UID) and tamper indications schemes for international safeguards applications [1]. New materials, including coatings and heterostructures open up the possibility of low cost fabrication of in-field verifiable coatings that can provide protective features and optical responses as a verifiable tool with applicability to tamper indication systems such as seals.

In order to strengthen verification schemes, the IAEA has anticipated the authorization of laser surface authentication (LSA [2]) for the verification of existing metal seals [3]. In addition, they have recommended the development of an easy to use and inexpensive active-electronic seal, along with the establishment of an effective capability to assess the seal system vulnerabilities. LSA utilizes the random speckle patterns which are formed by shining a laser on the surface of an object. It can read the unique "fingerprint" inherent in certain manufactured items by mapping microscopic variations across the surface of a range of materials, including paper, plastic, metal and ceramics. It is therefore imperative that the material, surface preparations and potential coatings that are being developed are compatible with this technique. Compatible transparent coatings can be employed to protect the surface features and include additional functionality such as tamper indication. SFC will serve as a first layer of protection for authentication and would allow in-situ verification of the item.

Researchers at the Savannah River National Laboratory (SRNL) are investigating the science of SFC as a versatile tamper indication technique that may be applied to a variety of materials, containers and equipment. All of these are vulnerable to tampering when fielded. It is envisioned that a SFC applied to the material or system (i.e. UF_6 cylinder, camera housing, or

seal) can allow an IAEA inspector to verify the authenticity of the item in-situ and extract information that can indicate whether tampering has occurred.

SMART FUNCTIONAL COATINGS (SFC)

A smart functional coating (SFC) is a system that can perform as a sensor or actuator by its capability to respond to physical, chemical, or mechanical stimuli. Changes in properties and structure can then be verified by a readable signal. The integration of functional materials such as rare earth dopants, inorganic, and polymeric coatings is being investigated to produce smart materials that combine photon stimulation with other properties that may respond to external conditions. SFC can act in a passive or active mode. In an active mode, it may be integrated into various elements including sensors, actuators, control algorithms, control hardware, and structural members that make up a complete smart system. Some of the benefits of smart coatings include the capability to respond to physical, chemical or mechanical stimuli by developing readable signals, and changes in properties and structure, in response to a change in environmental conditions. The use of rare earth dopants when combined with chemical solution deposition techniques provides a visual, identifiable detection method by a stimulus-response mechanism or photo-stimulation. The response is the emission of a characteristic wavelength associated with the state of the system. For sensors based on *color* response, the response may be visible color change, fluorescence, or phosphorescence as a result of a variety of stimuli. This simple, in-situ method of detection can provide to the inspector information for verification of the state of the system. Examples of such systems are summarized in.

One of the largest advantages of coating deposition by solution methods is the independence from the geometry of the substrate. Solutions can be deposited onto a variety of substrates such as ceramics, plastics, or metal by well-known methods including spin coating and dip coating. Solutions can be cast into a mold, and with further drying and heat-treatment, dense ceramic or glass articles with desired properties can be formed [4,5]. For example the reduction of the particle size well below the wavelength of visible light (~ 0.5 μm or 500 nm) eliminates much of the light scattering, allowing fabrication of a translucent material-a key factor for LSA compatibility.

Application to safeguards

Containment verification is a high priority for the international safeguards community. Nuclear material containers, equipment cabinets, camera housing, and detector cable conduits are all vulnerable to tampering or counterfeiting when fielded. In many cases, it is very difficult to distinguish counterfeit items from genuine products. SFC's applied to genuine materials surfaces allow the inspector to identify the item in-situ and extract information that can be used for continuity-of-knowledge. Additional advantages of smart coatings include: i) incorporation onto almost any surface, ii) the potential to incorporate active dopants for enhanced safeguards, verification and monitoring, iii) non-intrusive methodology for UID, iv) easily tailored for process or facility specific applications.

Table 1. Smart Polymeric coatings containing functional colorants (adapted reference [6]).

Sensor type	Sensing mechanism	Stimulus	Response
pH indicator	Ionic form of different color	pH change	Color
Fluorescence probe	Change in fluorescence intensity	Sorption, diffusion	Fluoresnce
Colorimetric dye	Colored metal complex	Heavy metal, radioactive contamination	Color change
Fluorescent polymer fiber, reactive sensor	TNT binds to receptor on chromophores, reducing signal, nerve gas reacting with sensor	TNT, nerve gas presence	Quenching fluoresnce
Conducting polymer	Switch between charged and neutral state. Change in surface conductivity or impedance	Oxide layer formation	Optical Absorbance, change in conductivity or electrical properties

EXPERIMENTAL

Material Selection

Transparent films prepared by chemical solution deposition methods based on alumina and silica were selected due to the ease of preparation, optical properties, ease of incorporation of dopants such as rare earth elements or nanoparticles, nontoxicity, scalable processes that do not depend on the object geometry, and the compatibility with ceramic materials of interest for the seal body.

Silica gel is the most common type of gel and the most extensively studied and used [4,7]. It is granular, vitreous, porous form of silicon dioxide made synthetically from sodium silicate. Despite its name, silica gel is a solid. It is a naturally occurring mineral that is purified and processed into either granular or beaded form. It allows the construction of materials that let light into buildings but trap heat for solar heating. It has remarkable thermal insulative properties, having an extremely low thermal conductivity.

Alumina gels can be synthesized using aluminum oxide [8], chlorides or nitrates. These gels are used typically as catalysts, especially when "metal-doped". Nickel-alumina gel is the most common combination. Alumina are also being considered by NASA for capturing of hypervelocity particles; a formulation doped with gadolinium and terbium could fluoresce at the particle impact site, with amount of fluorescence dependent on impact energy. By controlling synthesis conditions carefully, the sol morphology can be directed toward weakly branched polymeric systems or to particulate systems [9]. Important process parameters are water content, the solvent, the catalyst used and its concentration, and type of alkoxide used [4,10].

Selection of optical centers

Terbium (Tb^{3+}) and Erbium (Er^{3+}) were chosen as dopant due to the capability of dual excitation (UV and visible region) and compatibility with both alumina and silica matrix materials envisioned for film deposition [11]. Figure 1 shows the fluorescence spectra for 0.03 mol/L dopant concentration of (Tb^{3+}) and Erbium (Er^{3+}) in ethanol when excited with 375 nm UV light. Tb^{3+} is of particular interest due to the high intensity of emission (peak at 550 nm). Er^{3+} is known to have a strong emission in the visible and infrared region at 1540 nm that can serve as a hidden signal.

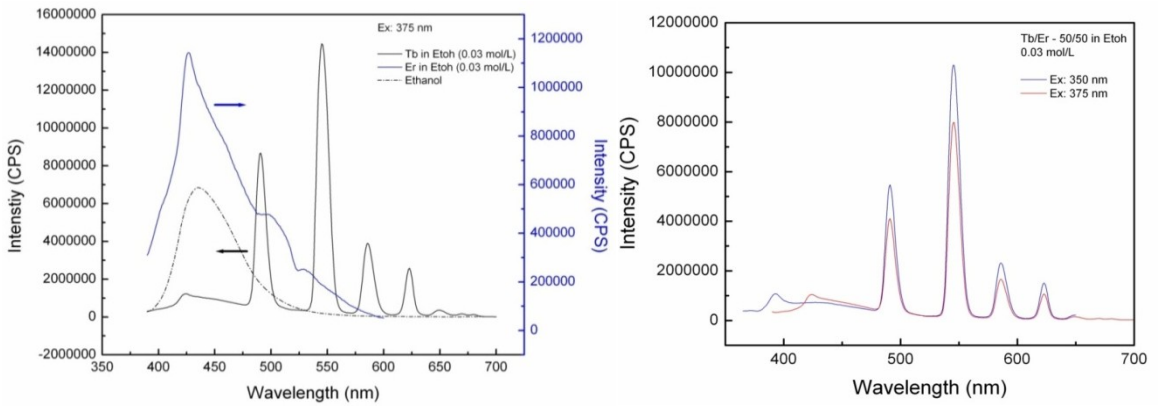

Figure 1. Comparison emission spectra of Er^{3+} and Tb^{3+} in ethanol [12].

Mixture of dopants can also be employed as method to increase the complexity of the coating. Mixtures of dopants in ethanol with a 50/50 ratio of Er^{3+}/Tb^{3+} display spectral features shown in Figure 1. The intense Tb^{3+} peak at 555 nm and 493 nm serves to mask the Er^{3+} emissions at 426 and 575 nm. A casual observer examining the fluorescence of $Tb^{3+}$and Er^{3+} mixtures in the visible region may conclude that only Tb^{3+} is present. If tampering is thought to have occurred, an examination of the broad range optical response of the seal can indicate if a counterfeit fluorescent coating was applied. Excitation and emission lines of selected dopant are summarized in Table 2.

Table 2. List of selected: their excitation and emission lines.

PSL precursor	Absorbs in	Emits in	λ_{ex} (nm)	λ_{em} (nm)
Erbium [13]	UV, Visible, IR	UV, Visible	377 488 520	426 575 617
Terbium [11]	UV	Visible	350	493, 539, 555, 585, 623

Method of Preparation

Amongst the different techniques available, the sol-gel method seems to be the most attractive one due to coating on the desired shape and area, easy to control of doping level, solution concentration and homogeneity without using expensive and complicated equipment when compared with other methods.

Undoped and Er^{3+}-doped alumina and silica were prepared by sol-gel method. All reagents were obtained from Sigma Aldrich. Alumina sol was obtained from aluminum sec-butoxide (ASB) in excess of water and by implementing the Yoldas process [14,15]. HNO_3 was used for peptization. The molar ratios of $ASB:H_2O:HNO_3$ used were 1:110:0.07. The silica sol was prepared by reacting tetraethoxysilane (TEOS) and water in ethanol (EtOH) as a mutual solvent following the procedure of Lenza and Vasconcelos [16]. HNO_3 was used as catalyst. The molar ratios of $TEOS:H_2O:EtOH:HNO_3$ used were 1:6:10.085. The Er^{3+}-doped sol were obtained by adding a solution of $Er(NO_3)_3$ in EtOH in sufficient amount to give a molar ratio of 0.1 as metal ion per alumina or silica. Undoped and Er^{3+}-doped sol samples were removed by pipette and deposited into quartz slides to form a thick film or by spin coating (200 – 800 rpm, 15 s) to form thinner films. The coated quartz slides were allowed to cool to room temperature and left to dry, at least 24 hrs.

ANALYSIS

Raman Spectroscopy

Raman spectroscopy is a useful technique for the identification of a wide range of substances – solids, liquids, and gases. It is a straightforward, non-destructive technique requiring no sample preparation. Raman spectroscopy involves illuminating a sample with monochromatic light and using a spectrometer to examine light scattered by the sample. Raman spectrum can be further utilized for map the distribution of dopants or additive to the gel, and cane employed as a method for material authentication. Raman scattering investigation was carried out in alumina and silica sol-gel, synthesized by Yoldas process, as function of rare earth concentration in the gel. Raman spectra were obtained at room temperature using a JASCO NRS5100 micro Raman spectrometer. An argon laser operating at 532 nm was the excitation source. The laser power at the sample was approximately 8 mW. We used an instrumental bandwidth of 2.1cm cm^{-1} focusing in the surface of the gel as deposited in a corning glass and air dried (>24 hrs) in a single point using a 20X optical objective. Each sample was scanned for a total of 30 sec.

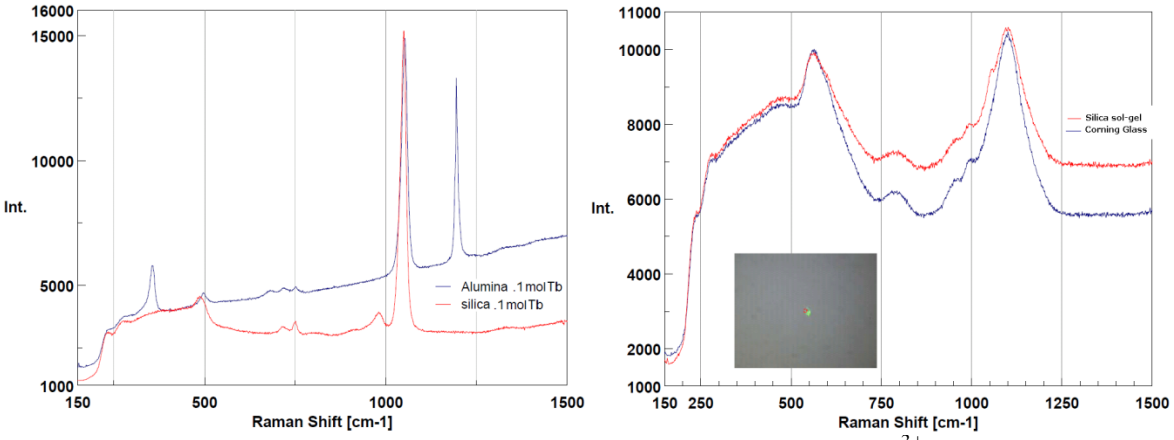

Figure 2. Raman spectra of silica and alumina sol-gel doped with Tb^{3+} (left) and Raman spectra of silica and corning glass (right).

Alumina-Gel

The Raman spectra of alumina samples doped with 0.1 mol Tb^{3+} after < 48hrs curing at room temperature are given in Figure 2 and Figure 3. Spectral bands associated to crystalline boehmite (AL-OH) [17,18], at 751, 681, 497, 369, 272, and 238 cm^{-1} were identified. Similar to the Si-gels spectrum an intense and sharp band at 1049 cm^{-1} is observed and is assigned to NO^{3-} vibration [19]. An unidentified sharp peak in the region of 1195cm^{-1} was identified in the alumina samples dope with Tb and is preliminary assigned to C-O- stretching band. It is known that carboxylic salt (C-O-C) have very strong characteristic bands in that region [20] and they double ~1050 cm^{-1}, a band that is also present in the Raman spectrum. A further evaluation of this region including IR spectroscopy will be needed to confirm the origin of this peak.

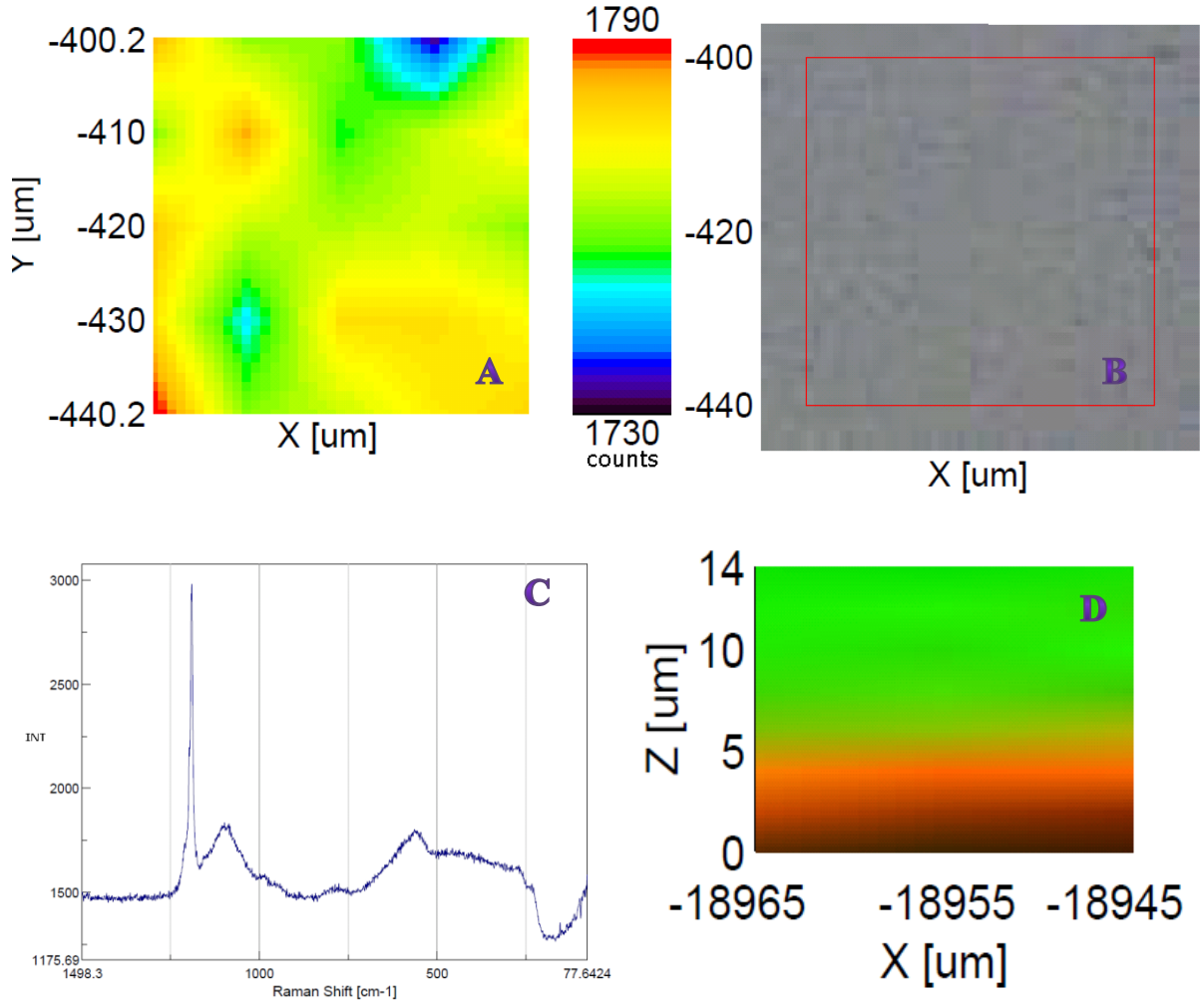

Figure 3. Raman map of alumina left and optical image of area scanned (40 x 40 µm) film deposited by spin coating (400rpm, 15 sec) in corning glass substrate. Color charge showing slightly variation (4%) in counts in the intensity Raman band. Figure Z map of alumina film deposited by spin coating (400rpm, 15sec). Red color indication Al-O bands against Si-O bands (green)

Silica-Gel

In order to facilitate the analysis of the experimental data of the Raman spectrum of corning glass and the sol-gel silica are shown in Figure 2. Raman spectra of Tb^{3+} (0.1 mol) doped alumina and silica are shown in same figure. The spectra of the silica gel show characteristic Raman at (~1180, ~1080, ~800, ~430 cm^{-1}) of fused quartz [21]. The spectrum of the sample [< 48hrs h] shows a broad band ranging from 250 to 500 cm^{-1} is assigned to the SiO_4 tetrahedral deformation vibrational mode. Characteristic band related to OH stretching vibration of Silanol groups at about 980 cm^{-1} due to the Si-O stretching vibration were also identified. The intense and sharp band at 1050 cm^{-1} is assigned to the C-O stretching vibration and is due to the presence of Si-O-CH_3 groups, originating from TEOS and to the presence of ethanol [22]. The broad band ranging from 250 to 500 cm^{-1} is assigned to SiO_4 tetrahedral deformation vibrations [23]. The sharp band at 490 cm^{-1} is due to the vibration of a O_3Si-OH tetrahedral [24]. Some weak bands appear between frequencies of 500 and 700 cm^{-1} indicating the presence of a small amount of partially hydrolyzed TEOS. A broad band centered at 800cm^{-1}, is assigned to Si-O-Si network vibration. Peaks at 980 cm^{-1} attributed to Si-OH stretching modes were also detected [25]. the spectrum obtained in the Tb and Er doped silica is similar to those obtained for undoped silica gels prepared under acidic conditions [26]. The Raman spectra of both silica and alumina gel have a luminescence background often observed in xerogels.

Figure 4 shows a Z (depth profile) map of silica film deposited by spin coated methods (400 rpm, 15 s) using as reference the 500-700 cm^{-1} region of associated with Si-O-CH_3 groups that are well known in the literature [27]. The estimated silica films ~5 microns.

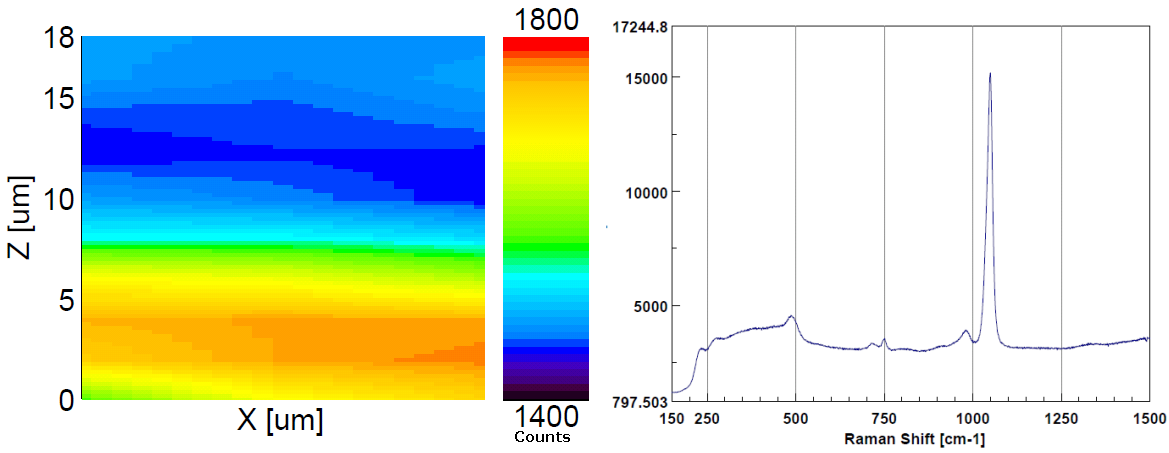

Figure 4. Raman Z map of deposited silica gel in quartz substrate by spin coating method (400 rpm, 15 s).

Scanning Electron Microscope and Energy dispersive X ray.

Electron microscopy forms the most widely used surface characterization methods. Scanning electron microscopy (SEM) provides information on the appearance, morphology and topography of the sample surface and near surface. SEM when combined with Energy Dispersive X-Ray spectroscopy (EDS) can be powerful tool for elemental identification and elemental

surface mapping. Advances in technology and miniaturization have made SEM available in small portable units that may allow field verification and analysis of samples.

Scanning electron microscopy (SEM) compositional (BSE) and topological analysis was employed to determine homogeneity and surface features of the sol-gel. BSE imaging is highly dependent on the atomic number Z and provides visual identification based on contrast of phases within the material. The higher the atomic number Z the brighter the resulting image, thus, the contrast is essentially a "chemical" contrast dependent on the atomic number Z and relative difference in densities of phases formed in sol-gel. SEM – BSE imaging was accompanied by the use of energy dispersive spectroscopy (EDS) for elemental identification and elemental composition mapping. The SEM used was a Hitachi TM-3000 (bench top scanning electron microscope) equipped with an energy dispersive spectroscopy (EDS) Bruker Quantax-70. EDS mapping creates an elemental image of the SEM image. This creates a distribution of the main elements and phases. The EDS system enabled the acquisition of x-ray data to confirm the elemental composition and provide qualitative/quantitative information of element distribution and atomic weight percentage on the region of interest. The combination of the data from these two techniques was used for elemental qualitative/quantitative analysis. While EDS combined with SEM is a powerful tool to characterize the samples, this method alone does not provide crystallographic orientation of the phases or oxidation states of the phases constituents. Regardless, it provides qualitative and quantitative analysis that can be used to determine the stoichiometry (or ratio) of elements present in an area of interest or phase. The examined samples were prepared by spin coating of the sol-gel (400 rpm, 15 sec) on a corning glass microscope slide. Figure 5 shown typical results of air dried (>24 hrs) sol-gel. Homogenous, crack free films were observed in samples at magnification from 180 – 1000X. Small features ~10 micron size were identified and possible related to impurities or dust at the surface of the glass during spin coating.

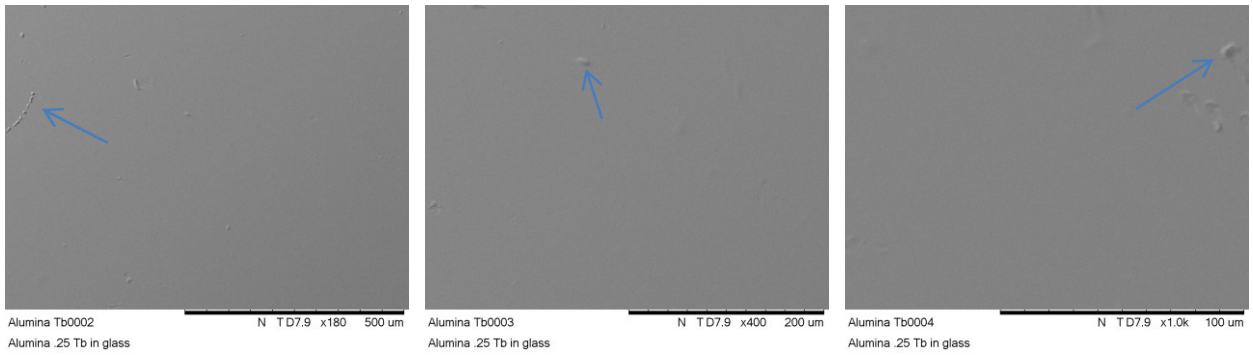

Figure 5. SEM micrograph (topography mode acc V-15 keV wd-7.9) of synthesized alumina gel deposited in corning glass surface by spin coating methods (400 rpm, 15 sec). Magnification from left to right 180X, 400X and 1000X.

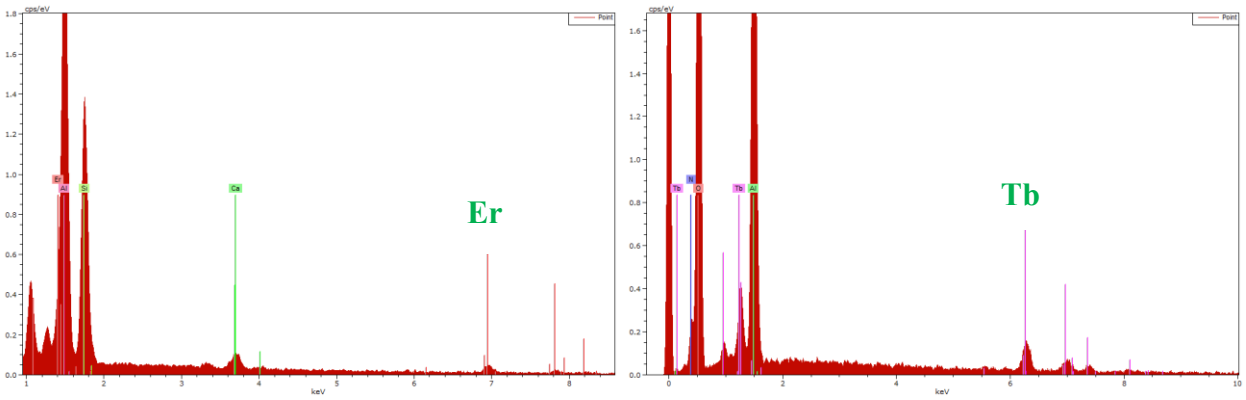

Figure 6. Energy dispersive spectrum of synthesis alumina Sol-Gels doped with Er^3 and Tb^3.

EDS elemental analysis Figure 6 and EDS mapping were used to determine the elemental composition of the sol-gel and the identification of dopants. Elements in the sol-gel Al, Si, O, N, were identified by EDS. Rare earth dopants Er and Tb were also identified in the sol-gel. Based on the SEM and EDS examination, the dopants were homogenously distributed in the bulk specimen.

UV-VIS

Ultraviolet and visible (UV-Vis) absorption spectroscopy is the measurement of the attenuation of a beam of light after it passes through a sample or after reflection from a sample surface. Absorption measurements can be at a single wavelength or over an extended spectral range. Ultraviolet and visible light are energetic enough to promote outer electrons to higher energy levels. Since the UV-Vis range spans the range of human visual acuity of approximately 400 - 750 nm, UV-Vis spectroscopy is useful to characterize the absorption, transmission, and reflectivity of a variety of technologically important materials, such as pigments, coatings, windows, and filters. Due to the compact size and easiness of operate handheld UV-Vis system have been employed in a variety of application including food, drug and coating inspection.

UV-Vis absorbance and percentage of transmission measurements were conducted on silica an alumina doped films spin coated in glass slides. A spectrophotometer with CCD array detector (Si Photonics 440), housing a deuterium and tungsten source for both ultra violet (300 - 450nm) and visible (450 nm - 950 nm) excitation were used. Examination of the optical transmittance of the films is show in Figure 7. Both film exhibit high level of transparency (< 85%) over the visible range (400 nm - 950 nm) Information concerning optical transmittance is importance in evaluating the optical performance of the deposited sol-gel. A high transparency in the visible region will be required in applications were LSA will be utilized to read the surface features of the underlying coating

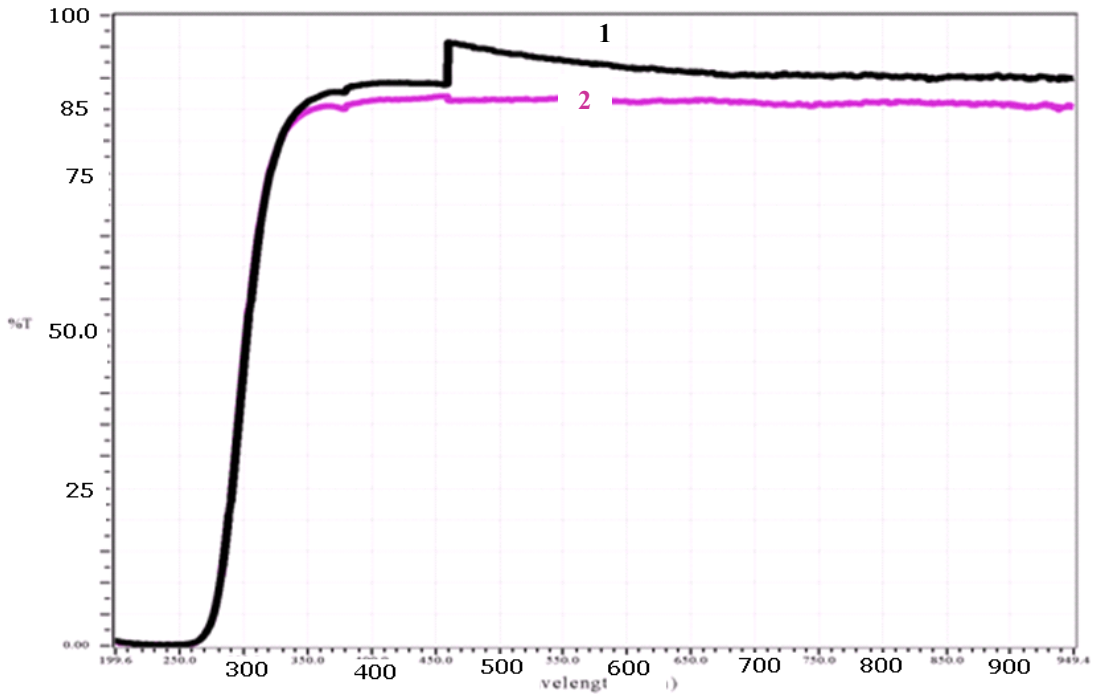

Figure 7. Optical transmission spectra 1- silica sol-gel and 2- alumina sol-gel deposited in corning glass slide by spin coating methods (400 rpm, 15 sec). Feature observed at 450 nm is related to transition of excitation source (deuterium-to-tungsten).

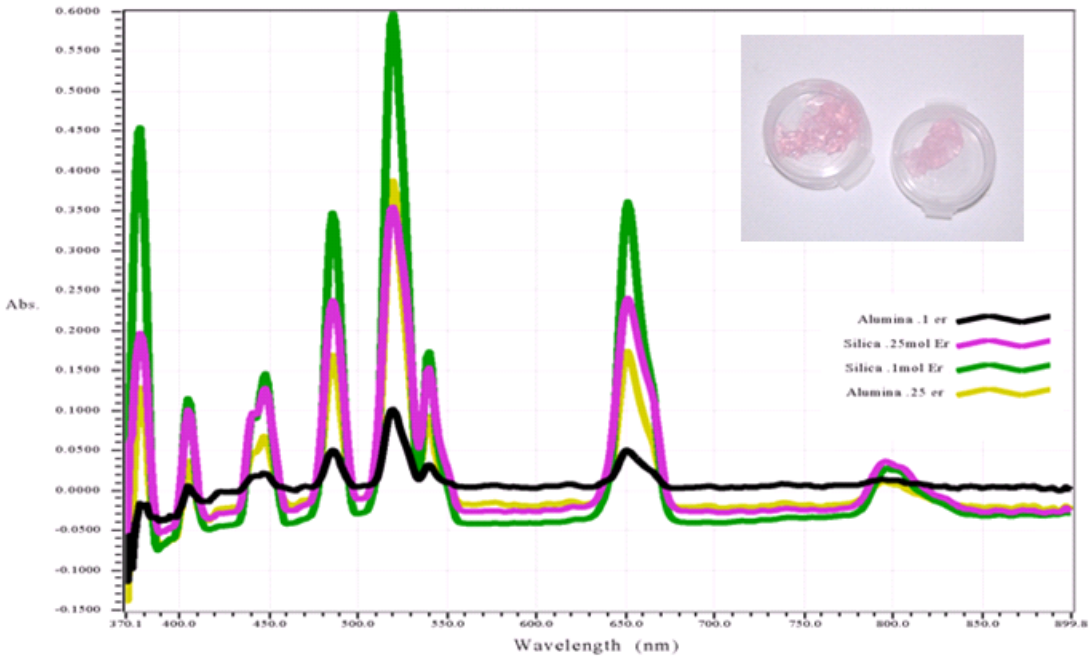

Figure 8. Optical absorption spectra of erbium doped silica and alumina sol-gel deposited in corning glass slide by spin coating methods (400 rpm, 15 sec). Absorption bands characteristics of Er^{3+} (377, 488, 520, 655 nm) were observed on the synthesized sol-gel. The insert figure corresponds to free standing silica sol-gel doped with Er^{3+}.

Because the absorbance of a sample will be proportional to the number of absorbing molecules in the spectrometer light beam (e.g. their molar concentration in the sample tube), dope silica and alumina sol-gel were prepared using the same dopants and dopants concentration.

Optical absorbance of silica and alumina gel as deposited in glass substrate is shown in Figure 8. Optical absorption band related to Er^{3+} (377, 488, 520, 655 nm) were observed both in synthesize alumina and silica sol-gels for Er^{3+} concentrations of 0.1 mol and 0.25 mol. Absorption spectra appear to be more pronounced for the same Er^{3+} concentration in silica gel than in alumina gel.

CONCLUSIONS

This paper highlights the research activities that have been conducted by SRNL in the areas of SFC, specifically materials selection and the development of SFC for use in a new generation of intrinsically tamper indicating ceramic seals (ITICS) [12] that may replace the current metal cup seal used by the international safeguard community. Synthesis of transparent coatings by chemical solution deposition methods including alumina and silica has been performed and deposited in quartz substrates. In addition, rare earth dopants that exhibit fluorescence have been successfully incorporated in the gel matrix and the optical properties have been characterized. Erbium (Er^{3+}) and Terbium (Tb^{3+}) have been identified as possible candidates for optically active dopants due to their optical response (UV excitation with visible emission), and in the case of Er^{3+} additional emissions band in the infrared region. Films fabricated from Er^{3+} and Tb^{3+} doped alumina and silica gels have been analyzed by visible absorption spectroscopy and have demonstrated a high degree of transparency in the visible range indicating potential compatibility with LSA. Alumina and Silica based coatings were fabricated by chemical solution deposition by hydrolysis and condensation reactions starting from a metal-alkoxide such as tetraethylorthosilicate (TEOS) and alumina sec butoxide. For solutions and coatings with an optical response it is of importance to understand the effect of dopant such as Er^{3+} and Tb^{3+}, their concentration, and their effects on the mechanical properties of the final film. The effects of additional parameter such as mechanical and chemical resistance need to be well understood in order to make solution methods a reliable and practical technology for safeguards applications. Future work will include the study dopant mixtures and sensitizer incorporated into the material that may enhance the optical response and increase the complexity of the final gel. Other optical centers including transition metals, can be also incorporated the film processing.

Techniques for the deposition of the Er^{3+} and Tb^{3+} doped alumina gels on alumina ceramics with tailored thickness in the micron range including dip coating and spin coating are currently being developed. The transparent nature of doped alumina gels indicate that fluorescent coatings may potentially serve dual roles of tamper indication through fluorescence as well as a protective surface layer compatible with LSA techniques. Fluorescent coatings applied to the seal body could provide the inspector with a quick and easy method to inspect seal integrity. The surface could potentially be inspected using a UV flashlight to check for defects in a continuous coating which could indicate cutting, drilling or other methods of seal penetration that would trigger in-depth seal verification. The science of SFC combine a low cost, easy to use and scalable technique that merge existing technology with new features that include multilayered protection with overt, covert and forensic-level security features.

Applications on seals

Seals are used in nuclear verification regimes to determine that material is neither introduced nor removed from a tamper-indicating container or that unattended monitoring equipment is not tampered with. Additionally, seals provide a unique identity (a tag) for the sealed container or item. Seal criteria include reliability, tamper-indication, *in situ* verification to reduce inspection effort, ease of evaluation of results, and ease of conclusiveness. These requirements are met by incorporating various layers of authentication and tamper indication, such as specially designed coatings. The IAEA in particular is interested in exploring new coating materials and techniques that would allow for quick and reliable verification of seal authenticity and integrity through characteristic optical measurements unique to the coating. Such innovations could serve the safeguards community by improving both the timeliness

REFERENCES

[1] IAEA Department of Safeguards. 2010-2011. R&D Programme.

[2] *LSA Technology*. Ingenia Technology [accessed Feb 23 2012]. Available from http://www.ingeniatechnology.com/the-lsa-technology/.

[3] LaMontagne, S. 2010. Overview of Containment/Surveillance for International Safeguards, in NNSA Office of Safeguards at the INMM International Workshop on Containment & Surveillance: Concepts for the 21st Century, June 7-11, at Oak Ridge, TN.

[4] Brinker, C.J., and G.W. Scherer. 1990. *Sol-Gel Science: The Physics and Chemistry of Sol-Gel Processing*. San Diego, CA: Academic Press, Inc.

[5] Schwartz, R.W., T. Schneller, and R. Waser. 2004. Chemical solution deposition of electronic oxide films. *Comptes Rendus Chimie* 7 (5):433-461.

[6] Feng, W., S.H. Patel, M.Y. Young, J.L. Zunino, and M. Xanthos. 2007. Smart polymeric coatings - Recent advances. *Advances in Polymer Technology* 26 (1):1-13.

[7] Hench, L.L., and J.K. West. 1990. The Sol-Gel Process. *Chemical Reviews* 90 (1):33-72.

[8] Lichtenberger, R., and U. Schubert. 2010. Chemical modification of aluminium alkoxides for sol-gel processing. *Journal of Materials Chemistry* 20 (42):9287-9296.

[9] de Lange, R.S.A., J.H.A. Hekkink, K. Keizer, and A.J. Burggraaf. 1995. Polymeric-silica-based sols for membrane modification applications: sol-gel synthesis and characterization with SAXS. *Journal of Non-Crystalline Solids* 191 (1-2):1-16.

[10] Lenza, R.F.S., and W.L. Vasconcelos. 2001. Preparation of Silica by Sol-Gel Method Using Formamide. *Materials Research* 4 (3):189-194.

[11] Ishizaka, T., R. Nozaki, and Y. Kurokawa. 2002. Luminescence properties of Tb(3+) and Eu(3+)-doped alumina films prepared by sol-gel method under various conditions and sensitized luminescence. *Journal of Physics and Chemistry of Solids* 63 (4):613-617.

[12] Mendez-Torres, A., D. Krementz, G. Weeks, K.S. Brinkman, J.E. Walker, D.L. Zamora, J.A. Romero, T.M. Weber, H.A. Smartt, and B. Schoeneman. 2011. Intrinsically Tamper Indicating Ceramic Seal (ITICS), in INMM 52nd Annual Meeting at Palm Desert, CA.

[13] Cabello, G., L. Lillo, C. Caro, G.E. Buono-Core, B. Chornik, and M.A. Soto. 2008. Structure and optical characterization of photochemically prepared ZrO2 thin films doped with erbium and europium. *Journal of Non-Crystalline Solids* 354 (33):3919-3928.

[14] Yoldas, B.E. 1975. A transparent porous alumina. *Ceramic Bulletin* 54 (3):286-288.

[15] Yoldas, B.E. 1975. Alumina sol preparation from alkoxides. *Ceramic Bulletin* 54 (3):289-290.

[16] Lenza, R.F.S., and W.L. Vasconcelos. 2001. Structural Evolution of Silica Sols Modified with Formamide. *Materials Research* 4 (3):175-179.
[17] Roy, A., and A.K. Sood. 1995. Phonons and fractons in sol-gel alumina: Raman study. *Pramana-Journal of Physics* 44 (3):201-209.
[18] Krishnan, R.S. 1947. Raman spectrum of alumina and the luminescence of ruby. *Proceedings of the Indian Academy of Sciences, Section A* 26:450-459.
[19] Doss, C.J., and R. Zallen. 1993. Raman studies of sol-gel alumina: Finite-size effects in nanocrystalline AlO(OH). *Physical Review B* 48 (21):15626-15637.
[20] Socrates, G. 2001. *Inrfrared and Raman Characteristics Group Frequencies: Tables and Charts*. 3rd ed. West Sussex , England: John Wiley and Sons.
[21] Bertoluzza, A., C. Fagnano, M.A. Morelli, V. Gottardi, and M. Guglielmi. 1982. Raman and infrared spectra on silica gel evolving toward glass. *Journal of Non-Crystalline Solids* 48 (1):117-128.
[22] Pucker, G., S. Parolin, E. Moser, M. Montagna, M. Ferrari, and L. Del Longo. 1998. Raman and luminescence studies of Tb3+ doped monolithic silica xerogels. *Spectrochimica Acta Part a-Molecular and Biomolecular Spectroscopy* 54 (13):2133-2142.
[23] Galeener, F.L. 1985. Raman and ESR studies of the thermal history of amorphous SiO_2. *Journal of Non-Crystalline Solids* 71 (1-3):373-386.
[24] Riegel, B., I. Hartmann, W. Kiefer, J. Gross, and J. Fricke. 1997. Raman spectroscopy on silica aerogels. *Journal of Non-Crystalline Solids* 211 (3):294-298.
[25] Murray, C.A., and T.J. Greytak. 1979. Intrinsic surface phonons in amorphous silica. *Physical Review B* 20 (8):3368-3387.
[26] Gottardi, V., M. Guglielmi, A. Bertoluzza, C. Fagnano, and M.A. Morelli. 1984. Further investigations on Raman spectra of silica gel evolving toward glass. *Journal of Non-Crystalline Solids* 63 (1-2):71-80.
[27] Lippert, J.L., S.B. Melpolder, and L.M. Kelts. 1988. Raman spectroscopic determination of the pH dependence of intermediates in sol-gel silicate formation. *Journal of Non-Crystalline Solids* 104 (1):139-147.